CrossMark

Finite Element Method Applied in Electromagnetic NDTE: A Review

Marek Augustyniak[1,2] · Zbigniew Usarek[1]

Abstract The paper contains an original comprehensive review of finite element analysis (FEA) applied by researchers to calibrate and improve existing and developing electromagnetic non-destructive testing and evaluation techniques, including but not limited to magnetic flux leakage (MFL), eddy current testing, electromagnetic-acoustic transducers (EMATs). Premium is put on the detection and modelling of magnetic field, as the vast majority of ENDT involves magnetic induction, either as a primary variable MFL or a complementary phenomenon (EC, EMATs). FEA is shown as a fit-for-purpose tool to design, understand and optimise ENDT systems, or a Reference for other modelling algorithms. The review intentionally omits the fundamentals of FEA and detailed principles of NDT. Strain-stress FEA applications in NDT, especially in ultrasonography and hole-drilling methodology, deserve as well a separate study.

Keywords Finite element method · Electromagnetic non-destructive testing · MFL · Eddy current testing · EMATs

1 Introduction

Non-destructive testing and evaluation (NDT, NDE or NDTE) attracts lasting attention driven by demands of reliability and economic service of engineering structures. Contemporary engineering—and NDT development in particular

—becomes increasingly associated with numerical modelling [1]. Among available modelling approaches, finite element analysis (FEA) has taken the lead in both academic and commercial applications. It is much more versatile than any analytical model. As compared to two major concurrent numerical approaches, i.e. boundary element method (BEM) and finite difference method (FDM), it is more intuitive, subject to less fundamental limitations (e.g. concerning unstructured mesh, nonlinearities or couplings) and is promptly available in several computer tools provided with a comfortable graphical user interface (GUI) and exhaustive user manuals.

Finite element analysis can complement and partially replace experimental ENDT for reasons listed below:

- the simulation allows for generating scenarios with a full control over all variables and phenomena
- it is impractical and in some cases unfeasible to measure electromagnetic parameters (magnetic induction, current density) inside a solid specimen [2], whereas these can be easily retrieved from FEA
- the measurement of a detailed distribution of the magnetic and/or electric field around an engineering object is time-consuming and requires painstaking data processing; by contrast, FEA software directly generates the resulting contour plots
- FEA tends to be more economic than experiment, especially when generating an array of results for subsequent inverse problem solution

Table 1 presents authors' attempt to arrange the techniques by the frequency range and the level of complexity. The latter variable corresponds to both the underlying physics and the practical difficulties in obtaining reliable results by either experiment or simulation. Any ENDT method,

✉ Marek Augustyniak
maugustyniak@mif.pg.gda.pl

[1] Gdansk University of Technology, 80-233 Gdańsk, Poland

[2] DES ART Ltd, 81-969 Gdynia, Poland

Table 1 A classification of ENDT methods by the range of frequency and relative complexity; numbers in parentheses indicate the relevant paragraph in the review

	passive MFL (5.3)	MBN and MAE (2.3)	Electromagnetic waves (5.1)
Complexity	MFL w. velocity effect (2.2)	Pulsed MFL (2.3)	EMAT (4)
	Static MFL (2.1)	RFECT (3)	ECT (3)
	Static	1 - 1000 Hz Frequency of excitation	kHz - MHz

including those located at the bottom of the classification, require careful calibration and interpretation. Therefore, the table contains only subjective indications. For example, remote field eddy current testing (RFECT) actually is superior in terms of complexity than the static MFL technique.
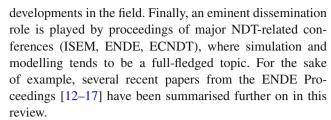
The choice of ENDT technique influences the strategy of finite element simulation. The key options to be selected in an electromagnetic numerical analysis are summarized below:

– time regime: static/harmonic/transient
– coupling (multiphysics): none/weak/strong
– boundary conditions: flux-parallel, flux-normal, fixed degree-of-freedom (DOF), coupling of DOFs
– nonlinearity: none/nonlinear B(H)/material anisotropy/ velocity effects
– element formulation (magnetic scalar or vector potential, edge-flux formulation)
– dimensionality (2D/2D-axisymmetric/3D)
– software (commercial/academic)

Simulation options listed above are described in more details in [6].

There are several commercial electromagnetic FEA software brands on the market, including MagNet, COMSOL, JSOL, MAXWELL, ANSYS Multiphysics, OPERA, FLUX and others. Their basic common functionality is computation of magnetostatics or electrostatics. Most codes can handle as well harmonic or transient problems involving eddy currents. Some tools are remarkable for the implementation of advanced functions, such as the magnetic hysteresis loop or a robust solution of a moving conductor induction. However, the market evolves rapidly, and the functionality of different tools tends to converge.

Important contributions of numerical modelling to ENDT are reported in three major groups of publications. Firstly, some monographs are available on the application of finite element method in electromagnetics [7–9]. In some of the books the electromagnetic NDT is the major topic [10,11]. Secondly, there are regular journals devoted to progress in NDT (incl. NDE, NDT&E, RNDE, "Insight" and others) containing both numerical and experimental

developments in the field. Finally, an eminent dissemination role is played by proceedings of major NDT-related conferences (ISEM, ENDE, ECNDT), where simulation and modelling tends to be a full-fledged topic. For the sake of example, several recent papers from the ENDE Proceedings [12–17] have been summarised further on in this review.

Bibliographic reviews on FEA applications in various engineering disciplines were systematically published by Mackerle (e.g. [3,4]), including an exhaustive bibliography on finite element modelling in NDT [5], encompassing the time span between 1976 and 1997 (plus an addendum reaching 2003). In the domain of electrical, magnetic an electromagnetic methods, that review focuses on ECT and the potential drop technique. Our review is complementary to the valuable Mackerle's work, offering up-to-date references and a discussion of specific features of modelling ENDT phenomena.

The following chapters present a review of finite element simulations applied in ENDT, followed by a discussion inspired by own experience in the field. In each chapter one ENDT method is briefly introduced, and some technical aspects of its finite element solution are given. Representative papers in the field are mentioned starting from the 1970ties. Alternative numerical methods and less typical ENDT applications are occasionally invoked. Although the Authors intended to provide a possibly comprehensive and balanced summary of the subject, this review remains a very individual and subjective insight into the vast amount of the published literature.

2 FEA in Magnetic Flux Leakage NDT

2.1 Static MFL

Static MFL methodology involves magnetizing a portion of a structure and recording the flux at the surface, in order to detect its anomalous spatial distribution. Usually a local magnetization close to saturation is required, because a leakage flux amplitude is generally proportional to the magnetization level. However, too high level of magnetization may lead to decrease a signal-to-noise ratio. The reason is an offset introduced by a background component of the signal. Most common sources of a magnetizing field, electromagnets or yokes with permanent magnets are used.

To design and optimize any MFL system a thorough understanding of magnetic circuit is required. The magnetostatic FEM solver is an efficient tool in MFL-related design and analysis [18]. The FEA solution of a MFL problem requires either a single nonlinear run (static analysis with B(H) curves) or a series of solutions at consecutive time points (transient analysis). The modelling can be 2D or 3D. The

material data consists of magnetization curves defined up to saturation ($\mu_R \sim 1.0$) and possibly electrical conductivities in the transient problem. The smoothness of B(H) curves can be essential for obtaining convergent solution [19]. The mesh density may be uniform, and the standard recommendation holds as to using the hexahedral element shapes whenever it is possible. The resulting vector fields (primary: B—the magnetic induction, and secondary: J—the current density) are vector real values. The numerical methods which cannot deal with nonlinear problems (e.g. BEM, FDM) are not suitable for MFL simulation [20]. Consequently, FEM is preferable in solving the equations governing electromagnetic field in MFL system.

One of the first numerical studies on the MFL defectoscopy including finite element calculation was published by Hwang and Lord in 1975 [21]. They predicted the magnetic field distribution around a rectangular slot on the surface of a circular ferromagnetic bar. The stress-flux correlations were numerically studied as early as in 1987 by Atherton and Czura [22]. They attributed the measured flux leakage over pipeline corrosion pits to stress-induced permeability changes and provided a 2D FEA to solve the inverse problem, i.e. to determine, how significant permeability change takes place in specimen.

The article [23] includes a study, in which apparently minor modifications of a model (inclusion of the detector assembly) produced dramatic qualitative changes of the results. It was demonstrated by 2D FEA, that anomalous leakage fluxes in the vicinity of pipe defects were non-linearly dependent on a defect depth. Further on, the constant H-excitation in a model gave significantly different results from a more realistic constant-B source.

In Atherton [24] a systematic study was performed towards the inverse problem solution of MFL over far side pipe grooves. The author demonstrated a strong linear correlation between anomalous radial flux densities calculated with 2D FEA and those obtained experimentally from 3D synthetic corrosion pits.

The following paragraphs summarise selected results of more recent research

The magnetostatic NDT was modelled with FEA by Al-Naemi, Hall and Moses [18]. The 2D (qualitative) vs 3D (quantitative) models generated and computed in MagNet software were compared against an experiment. The study reproduced the typical stray field behaviour over a defect in a flat plate. Although material data description is missing in the paper, one may presume that linear magnetic permeability was defined.

In Katoh et al. [25], the yoke-magnetization in MFL-testing was modelled with 2D static FEM modelling, using a self-developed software. The simulation was relatively basic, and did not aim at solving any inverse problem.

Another basic sensitivity analysis of the static magnetic circuit composed of a C-core magnet and the metallic specimen can be found in [26]. Linear magnetic permeability of the material, the core length and the spacing were modelled with COMSOL Multiphysics. Although the Barkhausen noise measurement was presented as the study's context, only the primary variables, i.e. magnetic induction B and field intensity H were computed.

Gaunkar et al. [26] redesigned the C-core magnetising setup with COMSOL FEA software, studying the influence of a core material, pole spacing and pole tip curvature. They employed a DC excitation and did not take saturation effects into account.

Babbar et al. [27] represented both the shape and residual stress influence on MFL patterns, over a slightly stamped (dented) plate. They used MagNet software to perform a static solution with a nonlinear, anisotropic B(H) curves. Interestingly, apart from the electromagnetic analysis, they started with structural FEA, subsequently dividing the plate into 13 discrete regions, having varying magnetic properties correlated with stress state. The MFL signal resulting from different stressed regions were studied separately and in combination with the shape effect. The authors found the excellent agreement between the FEA-derived and experimental MFL pattern.

Some papers with a precisely defined industrial context are invoked in the following paragraphs.

Christen et al. from Switzerland [1] examined the influence of steel wrapping on magneto-inductive testing of the main cables of suspension bridges. They employed MagNet software to create and solve a 3D model of a 2 m-long solid body with nonlinear B(H) characteristics. The set-up optimisation was sought, by studying the effect of a sensor lift-off and a magnetic excitation intensity. Based on the FEA results, a postprocessing procedure was proposed for separating and eliminating disturbance introduced by the steel wrapping.

In Gloria et al. [28] the pipeline corrosion defects were detected with a modified MFL, not requiring the saturation of a material. 2 and 3D numerical models were constructed using Gmsh and GetDP freeware finite element programs, and the geometrical parameters of the set-up were optimised. The simulation was compared favourably against an experiment.

A NDT group from India [29] examined with MFL steam generator tubes of a prototype fast breeder reactor. They created a 3D magnetostatic FEA model in COMSOL. They suggested a parallel use of MFL (for a detection of localised defects) and remote field ECT, sensitive to wall thinning, although no ECT simulation was provided.

A group from Queen's University, Canada [30], created a 3D magnetostatic model in MagNet software, in the context of pipeline MFL NDT. Effects of alignment of nearby pits

and stress-induced anisotropy were studied in a non-linear model.

Kikuchi et al. [31] examined the feasibility of NDT evaluation of magnetic properties and hardness of two-layered specimens by magnetostatic single-yoke probes. In spite of using a 2D approach in a simulation, they observed a good correlation between experimental and FEA-derived initial magnetisation curves for layered plates.

Coughlin et al. [32] examined the effect of stress on MFL responses from elongated corrosion pits in pipeline X70 steel excited with radial MFL set-ups. In this case the finite element 3D stress simulation was carried out, but no magnetic FEA.

The magnetic "signature" of cracks has been subject to relatively little research, as compared with the effect of stress or corrosion pits. Gao et al. [15] have published their resultss in ENDE Conf. Procs., claiming the competitiveness of their method of interpreting flux leakage near cracks over the standard 3D MFL approach. The standard 3D MFL, in turn, was numerically studied in [33], and an efficient yet accurate inversion algorithm in 2D was produced.

Some atypical usages of numerical simulation as a supportive tool for MFL are presented below.

Snarskii et al. [34] proposed a method of integral equations for the 3D solution of MFL over a surface defect in a plate of a finite thickness. They demonstrated the same accuracy as in FEA (Opera 3D software), but higher robustness. The demonstrated computation speed-up can be important when generating a large database of direct problem patterns, required for any inverse problem solution.

Mahendran and Philip [35] discussed a new magnetic emulsion to enhance visual magnetic NDT. Moreover, they included a comprehensive review of analytical methods of reproducing the field distribution, and pointed to some FEA-based studies, including that by Katoh et al.

Mukhopadhyay and Srivastava [36] tested efficiency of a discrete wavelet transform for a noise reduction MFL signal from a series of defects in a buried pipeline, and claimed the superiority of the method over its alternatives.

The observed trends and perspectives of further research are described in the last chapter of this preview.

2.2 MFL(V): Velocity Effects

High-speed non-destructive inspection systems using MFL method are in great demand in online inspection and defect characterisation, especially in pipeline and rail track maintenance [20]. The main component of these systems is an autonomous mobile device containing magnetic field sources and sensors, usually named pipeline inspection gauge (P.I.G.). Such a NDT set-up aims at deducing the shape and dimensions of a flaw, out of the voltage induced in a pick-up coil moving relatively fast (e.g. 1–10 m/s) along a studied structure.

MFL with the velocity effect shares the fundamental principles with the static MFL. An additional difficulty, in a signal interpretation and modelling, stems from the formation of eddy currents when an excitation source moves over or inside a pipeline. The first typical numerical approach to this problem is quasi-static, i.e. the simulation resembles the magnetostatic one, but an extra movement component is added to the governing equation (e.g. [37]). Another approach consists in representing the movement of the set-up over several time-steps, applying some type of electromagnetic coupling between the objects in the relative movement (e.g. [38]). Both the approaches encounter numerical difficulties (inaccuracy, unconvergence) as the relative velocity and material's magnetic permeability increase.

The start of finite element modelling of MFL with the velocity effect dates back to the 1980s (e.g. Shannon and Jackson [39] or Rodger et al. [40]). The effect of magnetizer velocity on MFL was subsequently simulated in 1992 by Nestleroth and Davis [41] using axisymmetric FEA, followed by works of Katragadda et al. [42,43].

Park and Park [44] analysed the velocity-induced eddy currents in MFL type ENDT, constructing a 3D finite element model. They designed a compensation scheme of the signal distortion, for velocities of the PIG reaching 5 m/s, coming up with a 'pure' defect-related signal, as if the probe is immobile.

Ireland and Torres [45] presented 2D finite element simulations in which a section of a pipe is magnetized along its circumference under both static and moving tool conditions. They employed the standard quasi-static approach with velocity equation component. They highlighted difficulties associated with maintaining a stable magnetic circuit when the set-up is moving. They noted, that a magnetic field profile is extremely complex under both stationary and dynamic tool conditions, and the repeatability of MFL defect patterns can be poor.

In another work [46] the same authors presented a preliminary research on a circumferential magnetizing set-up for pipeline inspection. They performed a dynamic FE analysis for the tool moving at 4 m/s. Both 2 and 3D models were generated, and the B(H) nonlinearity was taken into account. Several limitations and complexities of the method were indicated, including the difficulty to magnetize a pipe circumferentially and the dependence of the signal on the angular position of the set-up.

Li et al. [20] performed a simulation of MFL in a pipeline, with the set-up travelling at high speed, up to 30 m/s. The 2D model (quasi-static with velocity terms) is created in ANSOFT Maxwell. The authors discussed the signal-to-noise ratio and the optimum configuration of sensors.

Nestleroth and Davis [47] studied pairs of permanent magnets rotating around the central axis of a pipe in proximity of

its surface. The generated magnetic field was measurably disturbed over a defect. A finite element simulation, validated with experimental data, allowed for investigating a design space with various parameters such as a geometry, material properties, and excitation frequency.

The mentioned works are a representative, but non-exhaustive selection from amongst numerous studies on MFL with a moving source. New research results regularly emerge (e.g. [48,49]) and the subject is likely to attract lasting attention from the NDT community.

2.3 MFL(f): Frequency Effects

Judging from the number of publications and commercial implementations, the magnetic Barkhausen effect is the most important among micromagnetic phenomena applicable in ENDT. There is a significant amount of experimental articles aiming at elucidating the nature of MBN [50–52]. The micromagnetic modelling approaches to MBN representation were recently reviewed by Zapperi and Durin [53], and some results from stochastic (Monte Carlo) models were published as well [54]. However, relatively little has been done so far to develop macromagnetic or multiscale modelling schemes.

When using a C-core magnet in ENDT, replacing a DC excitation (typical for MFL) with a low-frequency (0–10 Hz) AC excitation allows acquiring additional data from the studied object, however the interpretation of signals is a challenging task. FEA plays an irreplaceable role in a comprehensive description of a time- and space-distribution of the magnetic induction within a studied object (plate, tube), which is impossible with any available analytical or experimental method. The FE solution of a magnetic field distribution inside a bulk ferromagnetic object is complicated by the fact, that excitation frequencies as low as 1 Hz generate a skin effect, which significantly disturbs the static field patterns [55–57]. Additional, special degrees of freedom (D.O.F.s) such as time-integrated electric potential may be necessary. Symmetry planes and initial conditions require special modelling approach. A time-transient scheme is preferred over a harmonic calculation, which usually leads to an incorrect representation of skin-effects due to the assumed B(H) linearity.

Augustyniak et al. [58] showed, that both the magnetic Barkhausen effect and the magnetoacoustic emission in a steel plate magnetized by a C-core electromagnet are significantly disturbed by eddy currents at excitation frequencies as low as 1 Hz. At least qualitative characteristics of these effects can be reproduced with FEA (ANSYS).

Another sensitivity analysis of the static magnetic circuit composed of a C-core magnet and the metallic specimen can be found in [26]. The material linear magnetic permeability, core length, and spacing were modelled with COMSOL Multiphysics. Although the Barkhausen noise measurement was presented as the study's context, only the primary variables, i.e. magnetic induction B and field intensity H were computed.

The Japanese group [59] focused on standardized samples used to assess the average induction within an object magnetized dynamically with a C-core set-up. They built a 3D model of the C-core and plates, made of different steels, and concluded, that the standard shim is applicable only to materials exhibiting a high magnetic permeability. Interestingly, they made use of a pseudo-nonlinear harmonic FEA instead of a fully-nonlinear time-transient solution, and found acceptable comparison against experiment.

A recent work [57] presents a detailed analysis of a time- and space-distribution of the nonlinear magnetic field inside a steel plate magnetized with a double-core electromagnet with a separate control of AC excitation currents on both branches. These results, obtained with transient electromagnetic FEA are complementary to the previous research by Nagata [60], who applied the method of boundary elements for calculation of magnetic fields and eddy currents induced by a pair of orthogonal C-cores.

Another step after having determined the magnetic field time- and space-distribution is reproducing the characteristics of Barkhausen effect or magnetoacoustic emission. In both ENDT methods there is an interaction of external, macroscopic excitation with microstructure, generating a series of short signals, either magnetic (MBN) or acoustic (MAE).

Spanish team [61] focused on angular anisotropy of MBN in pipes due to hot-rolling. Microscale FEM simulations of the magnetic flux density in an idealized steel sample containing the ferrite matrix and the pearlite bands were performed.

Pulsed MFL belongs to the methods under development. It bears some analogy to the acoustic borehole logging, i.e. the frequency content of the magnetic field resulting from a pulsed excitation carries information about the depth and extent of possible anomaly. Researchers from the University of Huddersfield [62] put forward a pulsed magnetic flux leakage technique (PMFL) for a crack detection and characterization. They indicated the limitations of a DC MFL, and suggested the superiority of PMFL, where the probe is driven with a square waveform and the rich frequency components can provide information from different depths due to the skin effects. They used FEMLAB (a transient, 2D, finite difference scheme) to study effects of surface and sub-surface cracks on the magnetic field.

Finally, an interesting hybrid MFL method called magneto-optic direct alternating imaging (MODAI) was studied by Novotny et al. [63]. They applied 2D harmonic FEA to demonstrate the feasibility of detection of defects by magneto-optic films. The optical effect was produced by either an AC or DC excitation. The authors investigated the

AC excitation at 10 kHz and claim the possibility of detecting small cracks, weak magnetic phases in nonmagnetic materials, corrosion pits, etc.
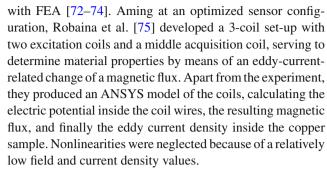
3 Eddy Current Testing (ECT)

Eddy current testing (ECT) is one of the most effective techniques for detecting cracks and flaws in conducting materials. In ECT devices, an alternate current flows in an exciting coil placed near a specimen suspected to have a flaw. Induced eddy currents affect a signal detected by the surrounding pick-up coils, influenced by a position, shape, and other characteristics of defects or variations of material properties [64]. The signal is usually analysed in terms of complex impedance plane trajectory. A magnitude and phase of a voltage drop induced in a detection coil is influenced by a variation of geometry and material parameters (μ, σ) of the studied object. The method applies equally to ferromagnetic and paramagnetic materials, including aluminium alloys. ECT techniques are widely (but not exclusively) used for the characterization of safety-critical components, e.g. employed in aeronautical and nuclear engineering.

A FEA solution of an EC problem requires a single harmonic linear run for each frequency of interest. A modelling can be axisymmetric, 2D or 3D. Material data consists of linear magnetic permeabilities and electrical conductivities of all the regions. The resulting vector fields (primary: J—current density and secondary: B—magnetic induction) are composed of real and imaginary parts, convertible into a magnitude or phase. Unlike in a harmonic structural analysis, resonances do not occur, so sampling of frequency at relatively large intervals is acceptable. A mesh density has to be refined within a sub-surface of an object in order to adequately represent the skin depth effect. An integration of B over the coil's cross-section and a subsequent time derivation produce an acceptable approximation of the coil's complex impedance, provided that the frequencies are limited so that the skin effect in the coil wire can be neglected. More discussion on numerical approaches to eddy currents can be found in [6]. Another valuable reference is the TEAM Workshop Project [65], involving FEA simulation benchmarks of several electromagnetic set-ups, including some EC-related problems.

First attempts to reproduce eddy current characteristics with FEA date back to late 70ties [66]. In the 80ties, intense research was conducted, led by Ida, Lord, Udpa and others [67–70]. Industrial case-studies were developed, e.g. the study by Palanisamy and Lord [71] focusing on a condenser tubing.

Design and validation of a new sensor configuration is one of leading topics in EC NDT and is often supported with FEA [72–74]. Aming at an optimized sensor configuration, Robaina et al. [75] developed a 3-coil set-up with two excitation coils and a middle acquisition coil, serving to determine material properties by means of an eddy-current-related change of a magnetic flux. Apart from the experiment, they produced an ANSYS model of the coils, calculating the electric potential inside the coil wires, the resulting magnetic flux, and finally the eddy current density inside the copper sample. Nonlinearities were neglected because of a relatively low field and current density values.

EC-sensor optimization was as well the main objective of the TEAM problem no. 27 [76], with eddy current NDT applied to some deep flaws. The aim was to optimize dimensions of a coil and an excitation current to have the highest level of a signal as possible. It is interesting to note, that the eddy currents were excited by a pulsed voltage excitation, and not a harmonic steady excitation.

In a study dedicated to ECT defectoscopy in airplane maintenance, Rosell and Persson [77] performed an experimental eddy current inspection of small fatigue cracks in Ti–6AL–4V sample and compare it against a finite element model. They noted, that as static loads were applied across the crack faces, electrical connections arise within the crack, which has a strong, detectable influence on the eddy current signal. The work focused on optimum method of incorporating this electrical contact effect into the simulation.

Apart from defectoscopy, the EC set-ups can be used to evaluate some material properties, including electrical conductivity, magnetic permeability, porosity, and tensile strength. One of basic examples is the TEAM benchmark no 15, concerning a non-destructive evaluation of materials with ECT. In another example, Ma et al. [78] created a FE model in Ansoft Maxwell representing a double-coil eddy current testing set-up over samples of Al foams manufactured by the sintering-dissolution process. Simulations gave a multi-frequency (10 Hz–1 MHz) response of the sensor/material geometry for 22 conductivities in the range of 0.1 to ~40 MS/m. The response was proportional to a change of mutual inductance of coils. The ultimate goal of both the experiment and the accompanying simulation was a reliable porosity evaluation with eddy currents.

In Augustyniak et al. [79], both a 2 and 3D modelling of a three-coil EC set-up over a boiler tube was presented and compared against an experiment. Standard practical factors—lift-off, wall thickness and tube diameter were studied with FEA at frequencies up to ~10 kHz. The proposed amplified differential signal was shown to carry information on the amount of magnetic ferrite phase forming on the tube during service.

Sablik and Augustyniak [80] proposed an application of EC sensors in the context of steel mills. Transient 2D

FEA time variation of a magnetic flux calculated in ANSYS was transformed by FFT into a set of harmonics, and their relative amplitudes were compared. Both the computation and experiment show an increase of the amplitude of the third harmonic with an increasing tensile strength of the plate.

Remote field eddy current testing (RFECT) is a major, industrially important variation of the standard eddy-current defectoscopy. While in conventional ECT, an exciter and detector coils are placed at the same location and operate at relatively high frequencies (1 kHz–10 MHz), in the RFECT both coils are several pipe diameters apart with a low frequency of operation from 40 to 160 Hz. The choice of a frequency reduces the skin effect and enables detection of flaws localized at the opposite side of the examined object, usually a pipe. In the 1980ties, RFECT phenomena were already experimentally observed successfully analysed using the finite element method. [81–84]. In Kim et al. [85], RFECT was applied to corroded gas transmission pipelines. Initial FEA studies showed that the rotating magnetic field PIG is sensitive to axially oriented tight cracks. Kasai et al. [86] performed an experimental and FEA 3D study in order to assess detectability of back-side flaws on flat ferromagnetic plates, in the context of corrosion of oil storage tanks. They modified the sensor and examined the signal itself as well as the signal-to-noise ratio. In the context of ENDE conferences, Mihalache et al. [17] developed a multifrequency RFECT algorithm applied specifically to the magnetic steam generation (SG) tubes of a fast breeder reactor (FBR). They determined algorithm parameters using proprietary 3D numerical FEA, and validated the concept with experimental measurements conducted on a small test tank.

FEA was successfully employed in non-standard EC techniques, including pulsed eddy-current defectoscopy [87] and stochastic approaches [88]. A special case was published by Kinoshita [89], who used MAXWELL 3D software to reproduce static and harmonic behaviour of magnetic field. The proposed 'electromagnetic impedance' NDT method was supposed to be able to detect fatigue progress of an aluminium alloy plated with ferromagnetic Ni–CO–P material. A permanent magnet in the simulation had a nonlinear anhysteretic B(H) relationship. The fundamental system relationship is determined between the coil's differential impedance and strains in the sample.

The modelling of pulsed ECT has been extensively covered in recent editions of ENDE conf. proceedings. Three examples have been selected for thes review. Zhang et al. [12] performed the 2D-FEM simulation in ANSYS reaching a successful correlation with an analytical model implemented in MATLAB. The problem at hand concerned pulsed eddy currents produced in a ferromagnetic plate with a flat bottom hole. Miorelli et al. [14] proposed a concept of surro-

gate models of Pulsed ECT, validating them in 3D using COMSOL. Finally, Xin an Lei [13] addressed a difficult problem of incorporating minor hysteresis loops into the calculation, in the context of measurement of pipeline wll thickness.

As popular and useful as it is, standard FEA is not the only approach to EC numerical prediction. Fetzer et al. [90] put forward a coupled FEM-BEM solution of the TEAM problem no. 8, concerning eddy-current NDT. They argued, that representation of the surrounding air with boundary elements greatly reduced computational effort.

Another alternative approach consisted in coupling FEA with some non-standard algorithms. For example, Ida [91] has recently proposed the coupling of FEM with surface impedance boundary conditions (SIBC), allowing elimination of the mesh in a conductor beyond the skin depth zone, thus increasing the speed of the solution without compromising accuracy. Similarly, Sabbagh and co-workers put forward an eddy-current NDT modelling scheme based on volume-integral equations [92–94]. The approach proved to be very successful in the computation of flaw responses in a number of simple geometries, but exhibited limitations in description of complicated surfaces.

More details on ECT methodologies with some references to numerical modelling can be found in [95].

4 EMATs (Electromagnetic Acoustic Transducers)

NDT based on EMATs is remarkable for its capability of detecting defects situated far away from an excitation source. The method can be considered as an extension of the standard ultrasonic defectoscopy particularly well suited for non-contact wave generation. EMATs work on nonmagnetic conducting materials (Lorentz force), or ferromagnetic materials (combination of Lorentz force, magnetostriction and magnetization forces). Optimization of EMATs in ferromagnetic materials is often accomplished using computational simulations that account for all the mentioned three main types of transduction mechanism. However, modelling the magnetization force is the least understood part of EMAT simulation and various authors often use controversial methods that lead to contradictory predictions. The discussion of these controversies has been avoided in this review, therefore only the papers considering the Lorentz force and/or magnetostriction are cited.

Although EMATs are broadband transducers and can function with pulsed excitation, they are often excited with a narrow band tone burst to maximize the signal-to-noise ratio, and the majority of simulations deal with a sinusoidal single-frequency excitation.

FE analysis of EMATs represents elastic wave propagation resulting from local application of magnetic fields. It is

usually composed of weakly coupled electromagnetic and structural (ultrasound) analyses. The electromagnetic FEA involved determination of a distribution of a static (bias) magnetic field, followed by a transient or harmonic calculation of time-varying B, eddy currents and Lorentz forces. Explicit solvers (ABAQUS Explicit, LS-DYNA, RADIOSS) are best suited for the structural part.

First numerical representations of EMAT date back to the 70ties, with the works by Thompson [96] and Kawashima [97]. Majority of subsequent works were oriented towards an improvement of set-up's performance by modification of geometrical parameters.

An EMAT was modelled in 2D and experimentally tested by Hao et al. [98] They generated a sequence of finite element calculations for a static magnetic field, a pulsed eddy current field, and resulting transient ultrasonic wave.

An exhaustive work by Mirkhani et al. [2] presented a practical numerical study aiming at enhancing the characteristics of an EMAT set-up (mainly signal-to-noise ratio). The FEA strategy included ANSYS EMAG computation followed by LS-DYNA 2D representation of ultrasonic waves. The pre-processor HyperMesh was applied at the latter stage, with the maximum mesh size equal to $\lambda/15$.

Wang et al. [99] proposed an enhancement to the previous FEA models of an EMAT, taking into account a dynamic magnetic field in a meander coil, coming up with the distribution of eddy currents, static magnetic field, Lorentz forces and resultant elastic waves. The FEA results corroborated with an experiment.

Dhayalan [100] presented a numerical analysis of multimode Lamb waves interacting with artificial defects and compares these calculations with measurements on a thin aluminium plate. They started with a 2D electromagnetic model (COMSOL software), reinserting resultant Lorentz forces into a subsequent ultrasonic computation (ABAQUS Explicit).

Kim et al. [101] employed ANSYS to reproduce the magnetic transducer consisting of a nickel grating, permanent magnets providing static bias magnetic field and a set of coils supplying or sensing a time-varying field. They used a topology optimization scheme over the permeable area of a transducer, in order to maximize both the static bias induction and the time-varying excitation field.

Dutton et al. [102] proposed a novel configuration of permanent magnets in an EMAT, consisting of two square magnets with similar magnetic poles facing each other. Effects of pole separation and lift-off were investigated. Both a simulation (FEMLAB) and an experiment consistently indicated an increase of the achieved magnetic induction in the region of interest by a factor of 1.8, as compared with a conventional one-magnet solution.

Huang et al. [103] applied ANSOFT FEA software to study optimum lift-offs in an EMAT system producing US waves at 250 kHz, designed so that only a magnetostrictive contribution took place in the specimen. They concluded, that the lift-off of a receiver could be very small, but the lift-off of a transmitter should be around 2 mm to ensure the stability of the system.

Zhou et al. [16] developed a FEM-BEM hybrid model to study the electromagneto-mechanical coupling influence on the simulated EMAT signals, considering the presence of the magnetostrictive force as well as the Lorentz force.

In spite of extensive published research, some fundamental controversies remained, including that defined by Ribichini et al. [104]. The question of major mechanism of elastic wave creation in ferromagnetic objects was asked: is this predominantly the Lorentz force, or rather magnetostriction? Using a COMSOL FE model, they demonstrate inconsistencies in previous studies and conclude that the Lorentz force usually dominates, except for highly magnetostrictive materials, such as nickel, iron–cobalt alloys or ferrite oxides.

5 Other ENDT Methods

5.1 Methods Involving Electromagnetic Waves

Although X-ray defectoscopy is one of the most popular NDT methods relying on electromagnetic wave propagation/absorption, it does not lend itself to standard FEA. Finite element simulation of the wave phenomena typically requires a mesh density of order of $\lambda/10$, so Angstrom-scale of Roentgen rays make reliable 3D calculations impossible for even most powerful computers available at present. However, waves of higher length (including microwaves) can successfully be simulated, which was demonstrated in some papers [105–107].

Electromagnetic wave propagation is the key phenomenon in electromagnetic emission (EME), sharing many features similar with the acoustic emission (AE). In case of a crack initiation and propagation, a temporary electric charge imbalance is a source of an electromagnetic wave measurable within a distance of a few millimetres [106].

Gade et al. [106] applied COMSOL commercial software to study the main characteristics of an EME sensor and obtained a very good correlation between the experiment and modelling. They claimed, that during the crack growth, an electromagnetic wave of acoustic frequency could be detected within a few mm from the surface of the studied epoxy resin object, and that EME could be a useful complementary tool for classic AE NDT.

It has to be underlined, that problems involving electromagnetic waves are more efficiently solved using other numerical approaches than FEA, such as Method of Moments (MoM) or finite difference in time domain (FDTD) [108].

5.2 ENDT Involving Static Electric Potential

NDT methods making use of an electric field as a primary factor are electrical impedance tomography (EIT) and electrical resistance tomography (ERT), being a particular case of the former. They do not involve any magnetic phenomenon and can be solved with FE (e.g. by Trefftz method) with electric potential as a single DOF. Contrary to ECT, the current sources in EIT/ERT are in electrical contact with a conducting object to be tested. The source field is produced by a direct current (DC) or by an AC source at very low frequency. Potential drops or local electric field measurements are often preferred to impedance or local magnetic field measurements, which are typical for ECT.

Although EIT/ERT was invented in the 80ties, the research results with a FEA background were first published after 2000.

Szczepanik and Rucki [109] performed a field analysis and investigated electrical models of multi-electrode impedance sensors. Two types of multi-electrode sensors, used in the impedance tomography systems, were simulated with FEA (COSMOSM software) in order to produce a simple, practical lumped-parameter model. Both the full (FEA) modelling and the simplified representation were successfully validated by the experiment.

Kahunen et al. [110] applied ERT to 3D imaging of concrete. They used an in-house software for both the forward and inverse analysis. Acceptable solutions of the inverse problem in some benchmark set-ups were presented.

Albanese et al. [64] made an initial evaluation of the usefulness of FEA in solving direct and reverse problems in an electrostatic search for buried objects. They carried out two benchmark simulations and experiments. ERT was used to retrieve the shape of a thin crack, and subsequently the geometry of a column immersed in water. Genetic algorithms were used to solve the inverse problem.

Daneshmand [111] and his co-author modelled the EIT to solve a forward problem in a biomedical context (a human thorax). The technique had been studied using FEM or BEM by other authors, but the novelty consisted in proposing a hybrid FEM-BEM strategy, combining advantages of both.

5.3 Passive MFL (MMM)

The "passive" MFL (sometimes called MMM, from "Metal Magnetic Memory") is a relatively new concept (1990ties), replacing a controlled magnetic field source with the Earth's field. Claimed cost-effectiveness of a simple portable measurement set-up has to be weighted against low reliability, leading to false-positive or false-negative findings. In spite of the official industrial standardisation (ISO 24497), there is a shortage of fundamental studies, especially those demonstrating its aptness to detect and quantify stress concentrations.

Interestingly, the magnetic FEA, useful as it proved in the standard MFL research, has rarely been used to understand, calibrate and optimize the methodology of passive stray field technique. The only published applications of numerical magnetic analyses in this context are either non-conclusive [112], or bring forth arguments against the concept [113–115].

Zurek [112] presented a preliminary study of contactless magnetostatic stress measurements on an ring made of a plain carbon steel. The results were partially successful, because a limited number of strain gauges did not allow the exact determination of stress and strain changes on the external ring surface. Both the magnetostatic (FLUX2D) and structural FEA (NASTRAN) was performed.

Usarek et al. [114] investigated the influence of the Earth's magnetic field on the distribution of stray magnetic field of a S355 steel sample, either undeformed or plastically deformed. A simple 3D model generated spatial variation of normal and tangential B component in agreement with the experimental data. The article concluded, that a reliable analysis of the stray magnetic field signal required balanced consideration of several factors, such as geometry of the element, plastic strain, and both internal and external stresses.

In a follow-up study, Usarek et al. [115] aimed at the separation of the effects of notch, magnetic permeability and macroscopic residual stress on the MFL signal characteristics. Experimental, as well as magnetostatic FEA, showed that geometrical effect, related to the notch presence, as well as degradation of magnetic permeability in the yielded zone, were mainly responsible for the specific MFL distribution above the sample.

In Augustyniak and Usarek [113] the magnetostatic 3D FEA was applied to study the influence of concurrent factors (geometrical discontinuity, magnetic permeability and remnant magnetisation) on the field strength gradient, claimed by some MMM proponents as correlated with elevated residual stress. The sensitivity study revealed, that the field gradient did not carry enough information to allow solving of an inverse quantitative problem, so determination of stress levels with a magnetic passive stray field alone is impossible. The effect of residual stresses in the studied dog-bone sample was found to be play minor role.

The published works indicate, that too many uncontrollable factors make passive MFL (or "MMM") unsuitable for a reliable quantitative assessment of stresses or material degradation. Numerical analysis served in this case to demonstrate the ambiguity of signal recorded in the passive MFL, and helped to better define the scope of applicability of the method.

6 Summary and Perspectives

6.1 Research Trends

The reviewed papers include four types of correlation between the simulated and measured results:

– simulation not referred to any experiment [56,104]
– qualitative correlation with an experiment [74,75]
– relative quantitative correlation [106,117]
– absolute quantitative correlation [97,113]

Relative quantitative correlation is defined here as demonstrating the same per cent variation of modelled and measured signals, with differing baseline values, typical for 2D modelling. Often it is not possible to make a sharp distinction between relative and absolute correlation, as in [106], where the measurement is presented in terms of voltage, which naturally is influenced by tunable amplification factor. If no reference to an experiment is provided, the paper should clearly demonstrate the soundness of modelling assumptions, and ideally be succeeded by another, experimental work.

In general, finite element analysis serves in every domain of ENDT as a complementary tool for better visualisation and analysis of phenomena at play, set-up optimisation/calibration, and the means of populating a matrix of results for subsequent inverse problem solution. However, application of numerical analysis in each ENDT method exhibits some unique tendencies.
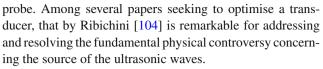
In static MFL, the range of simulation roles is broad: studying the stress or defect influence on stray field [27], optimising a set-up [1–26], and finally providing a reference solution for some special alternative numerical scheme [34]. One of the most advanced works in the field was that by Babbar [27], with a non-trivial geometry, non-uniform stress distribution and non-linear B(H) curve, and an excellent agreement between FEA and experiment.

In MFL with velocity effects the defectoscopy of pipelines and its numerical representation is the grossly dominating topic in scientific papers. One of most remarkable achievements was published by Park and Park [44], who put forward a compensation scheme for the signal from a moving PIG, of direct practical use for the operators.

Research on MFL with AC excitation usually aims at a realistic description of the dynamics of magnetic induction within a magnetic circuit composed of a C-core magnet and a studied ferromagnetic object.

In ECT, the leading topic is the design and optimisation of new sensor configurations. Most of the studies feature a well-defined industrial context (aviation, power plants, steel plants).

Simulations of EMATs usually aim at enhancing the signal-to-noise ratio by reshaping a excitation/detection probe. Among several papers seeking to optimise a transducer, that by Ribichini [104] is remarkable for addressing and resolving the fundamental physical controversy concerning the source of the ultrasonic waves.

As far as the "passive" MFL is concerned, several repetitions of Villari's experiment have been published, demonstrating that some change of material state (stress, plastic strain, fatigue) causes a variation of a stray field. The break-through presented in [116] (a function allowing to quantitatively deduce a residual stress from a stray field level) was later shown to be an overinterpretation [113].

6.2 Solutions of Inverse Problems

In NDT, the direct problem consists of the evaluation of a field perturbation at measurement probe locations, for a given exciting field and sample characterization (position, shape, material properties, stress state and defects). In the inverse problem, one has to find parameters of a sample assuming measurements and a forcing field as known quantities. Fast, accurate, and reliable simulation tools are necessary for a success of any inversion procedure.

There are three fundamental obstacles making the inverse problem solution in industrial ENDT challenging. The first one is the possible non-monotonic character of some measured parameters. The second consists in coexistence of several influence factors of a comparable impact on the measured signal. Relevant examples are the confounding conductivity and permeability factors in EC, or superposition of magnetic anisotropy and stress state in MBN [50]. The third problem is the complexity of any in-situ measurements, involving uncertainties higher than those associated with laboratory setting. These issues are discussed by [118], in the context of eddy current defectoscopy, and by Karhun et al. [110], who applied ERT to detection of internal defects in concrete structures. The numerical solution of the inverse problem is usually not unique, and it is sensitive to modelling errors and a measurement noise. Some attempts were unsuccessful, for example that by Roskosz [116], because of excessive number of influence variables as compared to the amount of measured data, which made the function inversion impossible [113].

The solution of inverse problems in ENDT requires some special strategies. One of these consists in obtaining 'richer' information from the studied object by applying several methods in parallel. For example, Sabet-Shargi et al. [119] present a multi-technique work focusing on accurate determination of stress state in hole-drilling method. They employed MBN, MFL and neutron diffraction measurements, and the structural FEA (ANSYS) was used to determine stress distributions in different situations. Szielasko [120] used the same strategy, in a probe designed for characterisation of high strength steels. Finally, Uchimoto et al. [121] employed an

original EMAT–EC dual probe to assess the extent of pipeline wall thinning.

Another approach to an ill-conditioned inverse problem relies on a sophisticated analysis of a signal [80], or switching from static to dynamic excitation [62]. In order to minimise the computation cost without compromising the accuracy, some authors propose a refinement of algorithms of problem inversion with design-of-experiment sampling, response-surface fitting [118], and neuron networks [122], The possible presence of several local extrema of the response function requires global optimization procedures, like genetic algorithms or artificial neural networks. The networks are first 'trained' using signals from a wide and possibly exhaustive range of defect shapes. To have a sufficient number of cases, training datasets are often generated using numerical simulations [122]. Genetic algorithms can efficiently be used in conjunction with FEM of the forward problem. In defectoscopy, a set of facets or elements forming a crack could be assuming as unknowns. In any case, to reduce the number of unknowns, some a priori assumptions have to be made on a class of defects under investigation [64].

Some successful solutions of inverse problems in ENDT were described already in the 80ties. In majority, they concerned ECT [123,124] and static MFL. In Atherton and Czura [22], there is an attempt to assess the order of magnitude of stress change from the magnetic stray field characteristics. The direct 2D problem is solved first, with an assumption of stress-permeability relationship, and then a computation of a stray field for a given non-uniform permeability. In Atherton [24], the corrosion pits are characterised on the basis of the MFL signal. The direct problem is solved first in 2D, with determination of MFL patterns of various defect geometries. Kim and Park [125] came up with an efficient algorithm of solving the MFL inverse problem, e.g. determining the 3D sizing of an axially oriented small crack from axial and circumferential MFL distributions within a pipe. Finally, one should note a mathematically rigorous paper by Tamburrion and Rubinacci [126], where a multi-frequency, EC scan over a conducting sample was successfully exploited to form a spatial map of the resistivity, thus indicating the location and allowing reconstruction of the shape of a flaw. The authors based on their previous experience with ERT, demonstrating that similar inverse algorithms can be applied to ECT.

6.3 Perspectives of Further Research

According to the presented literature review, FEA proved useful in all three constitutive domains of ENDT: defectoscopy, stress assessment and evaluation of intrinsic material properties. It has provided the possibility to simulate well-defined multi-factor scenarios and allowed to quantify phys-ical properties at any position where actual measurements could not be performed. FEA is particularly useful when an array of solutions of a forward problem is required, and analytical formulas are insufficiently accurate. Modelling can thus be a basis for solving essential inverse problems, i.e. determining unknown structural parameters (at both micro- and macro-scale) from the measurements. Numerical analysis has been as well successful at studying and enhancing actuators and sensors, esp. in ECT and EMAT techniques. What are the perspectives of further research?

The MFL technique with AC-excitation (mainly Barkhausen effect and MAE) is one of the most promising fields of research. Experimentally validated models, taking into account both micro- and macroscopic behaviour of the magnetic field inside the ferromagnetic object, are necessary. Assessment of bidirectional stress state, already possible with MBN, requires both more experimental and numerical studies to gain widespread acceptance and be reliably conducted.

In MFL with velocity effect, one awaits a validation and improvement of signal reconstruction scheme such as presented in [44] on a large series of industrial pipelines. Analysts and software developers should focus on overcoming numerical difficulties associated with increasing magnetic permeability and/or velocity of a probe.

In ECT there is a need for studies on non-uniform materials, especially those with a surface altered by corrosion or some intentional treatment (e.g. shot-peening). Some attempts can be found in [80] and [127]. One should note as well, that in most of papers the authors do not perform convergence considerations, i.e. the influence of meshing density is not studied. Allowable as it may be in case of MFL-related works, in case of eddy-current modelling the adequate number of elements through skin depth should be carefully determined lest magnetic field is artificially reduced within the material.

In static MFL, fundamental problems seem to have been solved, however it would be practical to extend the base of inverse problem solutions for arbitrary C-core parameters and arbitrary defects.

EMATs are the only field where simulation seems to have been sufficiently applied, and further developments (e.g. incorporating some minor nonlinear effects into the models) are not supposed to bring significant benefits.

Apart from the specific tasks listed above, some universal challenges may be identified, including:

- extension of ENDT methods to anisotropic materials (e.g. duplex steels, which exhibit strong difference in magnetic properties in orthogonal directions)
- implementation of robust element formulations with a stress-dependent hysteresis loop (preliminary results can be found in [128])

– development of some in-situ, 'intra-operational' FEA computation tools providing real-time support for measurements of complicated geometries

– creation of a NDT-dedicated FEA software, like specialist modules in ANSYS or COMSOL devoted to PCBs, MEMS or packaging

It should be clearly stated that computational simulations, regardless whether they exploit the finite element method or other schemes, can be used only when the underlying physics is well understood and the relevant material properties can be either measured or reliably estimated. For example, the passive remnant magnetic flux leakage (MFL) technique, which was misnamed by its original promoters as metal magnetic Method, cannot be relevantly studied by simulations because the underlying magneto-mechanical effect is far too complex and depends on far too many highly variable parameters.

Finally, the authors of this paper claim, that a top-quality study on ENDT with FE modelling should simultaneously be realistic, parametric, and industrial. 'Realistic' means involving a 3D, nonlinear approach taking into account necessary couplings (e.g. magneto-acoustic in MAE). A 'parametric' study enables construction of a matrix of direct solutions, being a pre-requisite for handling an inverse problem. Finally, 'industrial' work on a well-defined object of nontrivial geometry is preferable over an analysis of a generic sample in an idealised environment. Since the promising, well-structured ENDT case studies published in the 80ties, the prompt availability of the FEA software and dramatic increase of computing power have not always resulted in a proportional quality development of new studies. In particular, quantitative correlations between a simulation and industrial measurements are still rare, and attempts to solve practical inverse problems are in minority. More awareness in the ENDT community is necessary so that the potential of the electromagnetic FEA can be fully exploited.

References

1. Christen, R., Bergamini, A., Motavalli, M.: Influence of steel wrapping on magneto-inductive testing of the main cables of suspension bridges. NDT E Int. **42**(1), 22–27 (2009)

2. Mirkhani, K., Chaggares, C., Masterson, C., Jastrzebski, M., Dusatko, T., et al.: Optimal design of EMAT transmitters. NDT E Int. **37**(3), 181–193 (2004)

3. Mackerle, J.: Finite element and boundary element analyses of microwave, optical and acoustic waveguides. A bibliography (1994–1996). Finite Elem. Anal. Des. **28**(2), 165–175 (1997)

4. Mackerle, J.: Creep and creep fracture/damage finite element modelling of engineering materials and structures: a bibliography (1980–1999). Int. J. Press. Vessels Pip. **77**, 53–77 (2000)

5. Mackerle, J.: Finite-element modelling of non-destructive material evaluation: a bibliography (1976–1997). Model. Simul. Mater. Sci. Eng. **7**, 107–145 (1999)

6. Tang, K.C., Ellis, D.: Why Do Electromagnetic Finite Element Analysis?. NAFEMS Publishing, London (2009)

7. Bastos, J.P.A., Sadowski, N.: Electromagnetic Modelling by Finite Element Methods. Marcel Dekker, New York (2003)

8. Bastos, J.P.A., Sadowski, N.: Magnetic Materials and 3D Finite Element Modelling. CRC Press, Boca Raton (2014)

9. Jin, J.: The Finite Element Method in Electromagnetics. Wiley, Hoboken (2014)

10. Ida, N.: Numerical Modelling for Electromagnetic Nondestructive Evaluation. Chapman & Hall, London (1995)

11. Sabbagh, H.A., Murphy, R.K., Sabbagh, E.H., Aldrin, J.C., Knopp, J.S.: Comutational Electromagnetics and Model Based Inversion. Springer, Berlin (2013)

12. Zhang, Q., Wu, X., Li, J., Sun, P.: Analysis of pulsed eddy current testing for ferromagnetic metallic materials with flat-bottom hole defect. In: Chen, Z., et al. (eds.) Electromagnetic Nondestructive Evaluation (XVIII), pp. 95–102. IOS Press, Amsterdam (2015)

13. Xin, W., Lei, Y.Z.: Analysis of a pulsed eddy current testing method for ferromagnetic pipeline wall thickness determination considering minor hysteresis. In: Chen, Z., et al. (eds.) Electromagnetic Nondestructive Evaluation (XVIII), pp. 117–124. IOS Press, Amsterdam (2015)

14. Miorelli, R., Dubois, A., Bilicz, S., Theodoulidis, T., Reboud, C.: Simulation of pulsed eddy current testing via surrogate models. In: Capova, K., et al. (eds.) Electromagnetic Nondestructive Evaluation (XVII), pp. 120–127. IOS Press, Amsterdam (2014)

15. Gao, Y., Wang, P., Tian, G.: Numerical simulation of magnetic flux leakage for crack geometrical characterization based on spatial magnetic field vectors. In: Chen, Z., et al. (eds.) Electromagnetic Nondestructive Evaluation (XVIII), pp. 125–132. IOS Press, Amsterdam (2015)

16. Zhou, H., Yang, Z., Li, Y.: Numerical simulation of EMAT for structures of ferromagnetic material with consideration of electromagneto–mechanical coupling effect. In: Chen, Z., et al. (eds.) Electromagnetic Nondestructive Evaluation (XVIII), pp. 110–116. IOS Press, Amsterdam (2015)

17. Mihalache, O., Yamaguchi, T., Ueda, M.: Validations of multifrequency ECT algorithms for helical SG tubes of FBR. In: Capova, K., et al. (eds.) Electromagnetic Nondestructive Evaluation (XVII), pp. 109–119. IOS Press, Amsterdam (2014)

18. Al-Naemi, F.I., Hall, J.P., Moses, A.J.: FEM modelling techniques of magnetic flux leakage-type NDT for ferromagnetic plate inspections. J. Magn. Magn. Mater. **304**(2), 790–793 (2006)

19. Augustyniak, M., Usarek, Z.: Control of magnetic circuit parameters in quasi-static magnetic non-destructive testing. Part I: analytical and 2-D model. Zesz. Naukowe Wydz. Elektrotech. Autom. Politec. Gdan. **40**, 17–21 (2014). (Article in Polish)

20. Li, Y., Tian, G.Y., Ward, S.: Numerical simulation on magnetic flux leakage evaluation at high speed. NDT E Int. **39**(5), 367–373 (2006)

21. Hwang, J.H., Lord, W.: Finite element modeling of magnetic field/defect interactions. J. Test. Eval. **3**(1), 21–25 (1975)

22. Atherton, D.L., Czura, W.: Finite element calculations on the effects of permeability variation on magnetic flux leakage signals. NDT E Int. **20**(4), 239–241 (1987)

23. Atherton, D.L., Daly, M.G.: Finite element calculation of magnetic flux leakage detector signals. NDT E Int. **20**(4), 235–238 (1987)

24. Atherton, D.L.: Finite element calculations and computer measurements of magnetic flux leakage patterns for pits. Brit. J. Nondestr. Test. **30**(3), 159–162 (1988)

25. Katoh, M., Masumoto, N., Nishio, K., Yamaguchi, T.: Modeling of the yoke-magnetization in MFL-testing by finite elements. NDT E Int. **36**(7), 479–486 (2003)

26. Gaunkar, N.P., Kypris, O., Nlebedim, I.C., Jiles, D.C.: Optimization of sensor design for Barkhausen noise measurement using finite element analysis. J. Appl. Phys. **115**, 1–4 (2014)

27. Babbar, V., Bryne, J., Clapham, L.: Mechanical damage detection using magnetic flux leakage tools: modeling the effect of dent geometry and stresses. NDT E Int. **38**(6), 471–477 (2005)

28. Gloria, N.B.S., Areiza, M.C.L., Miranda, I.V.J., Rebello, J.M.A.: Development of a magnetic sensor for detection and sizing of internal pipeline corrosion defects. NDT E Int. **42**(8), 669–677 (2009)

29. Singh, W.S., Rao, B.P., Thirunavukkarasu, S., Mahadevan, S., Mukhopadhyay, C.K., et al.: Development of magnetic flux leakage technique for examination of steam generator tubes of prototype fast breeder reactor. Ann. Nucl. Energy **83**, 57–64 (2015)

30. Mao, W., Clapham, L., Atherton, D.L.: Effects of alignment of nearby corrosion pits on MFL. NDT E Int. **36**(2), 111–116 (2003)

31. Kikuchi, H., Murakami, H., Ara, K.: Feasibility study for nondestructive evaluation of magnetic properties and hardness of two-layered specimens by magnetic single-yoke probe. NDT E Int. **46**, 1–6 (2012)

32. Coughlin, C.R., Clapham, L., Atherton, D.L.: Effects of stress on MFL responses from elongated corrosion pits in pipeline steel. NDT E Int. **33**(3), 181–188 (2000)

33. Priewald, R.H., et al.: Fast magnetic flux leakage signal inversion for the reconstruction of arbitrary defect profiles in steel using finite elements. IEEE Trans. Magn. **49**(1), 506–516 (2013)

34. Snarskii, A.A., Zhenirovskyy, M., Meinert, D., Schulte, M.: An integral equation model for the magnetic flux leakage method. NDT E Int. **43**(4), 343–347 (2010)

35. Mahendran, V., Philip, J.: Naked eye visualization of defects in ferromagnetic materials and components. NDT E Int. **60**, 100–109 (2013)

36. Mukhopadhyay, S., Srivastava, G.P.: Characterisation of metal loss defects from magnetic flux leakage signals with discrete wavelet transform. NDT E Int. **33**(1), 57–65 (2000)

37. De Gersem, H., Hameyer, K.: Finite element simulation of a magnetic brake with a soft magnetic solid iron rotor. COMPEL Int. J. Comput. Math. Electr. Electron. Eng. **21**(2), 296–306 (2002)

38. Gay, S.E., Ehsani, M.: Parametric analysis of eddy-current brake performance by 3-D finite-element analysis. IEEE Trans. Magn. **42**(2), 319–328 (2006)

39. Shannon, R.W.E., Jackson, L.: Flux leakage testing applied to operational pipelines. Mater. Eval. **46**(2), 1516–1524 (1988)

40. Rodger, D., Karaguler, T., Leonard, P.J.: A formulation for 3D moving conductor eddy current problems. IEEE Trans. Magn. **25**(5), 4147–4149 (1989)

41. Davis, R.J., Nestleroth, J.B.: The effects of flux leakage magnetizer velocity on volumetric defect signals. In: Thompson, D., Chimenti, D. (eds.) Review of Progress in Quantitative Nondestructive Evaluation, vol. 14, pp. 491–498. Springer, Berlin (1995)

42. Katragadda, G., Si, J.T., Lord, W., Sun, Y.S., Udpa, S., Udpa, L.: 3D finite element methods for modeling MFL inspection of pipelines. In: Thompson, D., Chimenti, D. (eds.) Review of Progress in Quantitative Nondestructive Evaluation, vol. 15A, pp. 561–567. Springer, Berlin (1996)

43. Katragadda, G., Sun, Y.S., Lord, W., Udpa, S., Udpa, L.: Velocity effects and their minimization in MFL inspection of pipelines—a numerical study. In: Thompson, D., Chimenti, D. (eds.) Review of Progress in Quantitative Nondestructive Evaluation, vol. 14, pp. 499–505. Springer, Berlin (1995)

44. Park, G.S., Park, S.H.: Analysis of the velocity-induced eddy current in MFL type NDT. IEEE Trans. Magn. **40**(2), 663–666 (2004)

45. Ireland, R.C., Torres, C.R.: Finite element modelling of a circumferential magnetiser. Sensors Actuators A Phys. **129**(1–2), 197–202 (2006)

46. Ireland, R.C., Torres, C.R.: Challenges in circumferential magnetisation: a FEA point of view. In: Proc. IPC, pp. 945–955 (2004)

47. Nestleroth, J.B., Davis, R.J.: Application of eddy currents induced by permanent magnets for pipeline inspection. NDT E Int. **40**(1), 77–84 (2007)

48. Kim, H.M., et al.: Defect estimation of a crack in underground pipelines by CMFL type NDT system. In: Proceedings of International Conference on Electrical Machines and Systems, Busan (2013)

49. Wang, P., Gao, Y., Tian, G., Wang, H.: Velocity effect analysis of dynamic magnetization in high speed magnetic flux leakage inspection. NDT E Int. **64**, 7–12 (2014)

50. Lindgren, M., Lepistö, T.: On the stress vs. Barkhausen noise relation in a duplex stainless steel. NDT E Int. **37**(5), 403–410 (2004)

51. Kleber, X., Barroso, S.P.: Investigation of shot-peened austenitic stainless steel 304L by means of magnetic Barkhausen noise. Mater. Sci. Eng. A. **527**, 6046–6052 (2010)

52. Augustyniak, B.: Correlation between acoustic emission and magnetic and mechanical Barkhausen effects. J. Magn. Magn. Mater. **196–197**, 799–801 (1999)

53. Zapperi, S., Durin, G.: New perspectives for Barkhausen noise. Comput. Mater. Sci. **20**(3–4), 436–442 (2001)

54. Yamaguchi, K., Tanaka, S., Watanabe, H., Nittono, O., Yamada, K., Takagi, T.: Analysis of Barkhausen noise using Monte Carlo simulation for nondestructive evaluation. J. Mater. Process. Technol. **161**(1–2), 338–342 (2005)

55. Augustyniak, M., Augustyniak, B., Piotrowski, L., Chmielewski, M.: Evaluation by means of magneto-acoustic emission and Barkhausen effect of time and space distribution of magnetic flux density in ferromagnetic plate magnetised by a C-core. J. Magn. Magn. Mater. **304**, 552–554 (2006)

56. Augustyniak, M., Augustyniak, B., Chmielewski, M., Sadowski, W.: Numerical evaluation of spatial time-varying magnetisation of ferritic tubes excited with a C-core magnet. J. Magn. Magn. Mater. **320**, 1053–1056 (2008)

57. Augustyniak, M., Augustyniak, B., Piotrowski, L., Chmielewski, M.: Determination of magnetisation conditions in a double-core Barkhausen noise measurement set-up. J. Nondestruct. Eval. **34**, 16 (2015)

58. Augustyniak, B., Piotrowski, L., Augustyniak, M., Chmielewski, M., Sablik, M.J.: Impact of eddy currents on Barkhausen and magnetoacoustic emission intensity in a steel plate magnetized by a C-core electromagnet. J. Magn. Magn. Mater. **272–276**, E543–E545 (2004)

59. Kasai, N., Takada, A., Fukuoka, K., Aiyama, H., Hashimoto, M.: Quantitative investigation of a standard test shim for magnetic particle testing. NDT E Int. **44**(5), 421–426 (2011)

60. Nagata, S., Enokizono, M.: Numerical simulations and experiments of eddy current tests under various excitation methods. J. Mater. Process. Technol. **161**(1–2), 353–358 (2005)

61. Martínez-Ortiz, P., Pérez-Benitez, J.A., Espina-Hernández, J.H., Caleyo, F., Hallen, J.M.: On the estimation of the magnetic easy axis in pipeline steels using magnetic Barkhausen noise. J. Magn. Magn. Mater. **374**, 67–74 (2015)

62. Sophian, A., Tian, G.Y., Zairi, S.: Pulsed magnetic flux leakage techniques for crack detection and characterisation. Sensors Actuators A Phys. **125**(2), 186–191 (2006)

63. Novotny, P., Sajdl, P., Machac, P.: A magneto-optic imager for NDT applications. NDT E Int. **37**, 645–649 (2004)

64. Albanes, R., Calabró, G., Lombardo, G., Reitano, G., Fresa, R., Morabito, P.: Error bounds for inverse electromagnetic problems in soil mechanics. Math. Comput. Model. **37**(5–6), 603–613 (2003)

65. Testing Electromagnetic Analysis Methods. International Compumag Society. http://www.compumag.org/jsite/team.html. Accessed 30 Nov 2015

66. Chari, M.V.K., Kincaid, T.: The application of finite element method analysis to eddy current nondestructive evaluation. IEEE Trans. Magn. **15**(6), 1956–1960 (1979)

67. Ida, N., Lord, W.: A finite element model for three-dimensional eddy current NDT phenomena. IEEE Trans. Magn. **21**(6), 2635–2643 (1985)

68. Allen, B., Ida, N., Lord, W.: Finite element modeling of pulse eddy current NDT phenomena. IEEE Trans. Magn. **21**(6), 2250–2253 (1985)

69. Udpa, L., Lord, W.: Impedance and mesh structure considerations in the finite element analysis of eddy current NDT probe phenomena. IEEE Trans. Magn. **21**(6), 2269–2272 (1985)

70. Palanisamy, R., Lord, W.: Prediction of eddy current probe signal trajectories. IEEE Trans. Magn. **16**(5), 1083–1085 (1980)

71. Palanisamy, R., Lord, W.: Prediction of eddy current signals for nondestructive testing of condenser tubing. IEEE Trans. Magn. **19**(5), 2213–2215 (1983)

72. Nath, S., Wincheski, B., Fulton, J.P., Namkung, M.: Study of the new eddy current non-destructive testing sensor on ferromagnetic materials. IEEE Trans. Magn. **30**(6), 4644–4646 (1994)

73. Thollon, F., Burais, N.: Geometrical optimization of sensors for eddy currents. Non destructive testing and evaluation. IEEE Trans. Magn. **31**(3), 2026–2031 (1995)

74. Huang, H., Sakurai, N., Takagi, T., Uchimoto, T.: Design of an eddy-current array probe for crack sizing in steam generator tubes. NDT E Int. **36**, 515–522 (2003)

75. Robaina, R.R., Alvarado, H.T., Plaza, J.A.: Planar coil-based differential electromagnetic sensor with null-offset. Sensors Actuators A Phys. **164**(1–2), 15–21 (2010)

76. Dyck, D.N., Gilbert, G., Forghani, B., Webb, J.P.: An NDT pulse shape study with TEAM problem 27. IEEE Trans. Magn. **40**(2), 1406–1409 (2004)

77. Rosell, A., Persson, G.: Finite element modelling of closed cracks in eddy current testing. Int. J. Fatigue **41**, 30–38 (2012)

78. Ma, X., Peyton, A.J., Zhao, Y.Y.: Measurement of the electrical conductivity of open-celled aluminium foam using non-contact eddy current techniques. NDT E Int. **38**(5), 359–367 (2005)

79. Augustyniak, B., Chmielewski, M., Sablik, M.J., Augustyniak, M.: A new eddy current method for nondestructive testing of creep damage in austenitic boiler tubing. Nondestruct. Test. Eval. **24**(1–2), 121–141 (2009)

80. Sablik, M., Augustyniak, M.: Nonlinear harmonic amplitudes in air coils above and below a steel plate as a function of tensile strength via finite-element simulation. IEEE Trans. Magn. **40**(4), 2182–2184 (2004)

81. Lord, W., Sun, Y.S., Udpa, S.S., Nath, S.: A finite element study of the remote field eddy current phenomenon. IEEE Trans. Magn. **24**, 435–438 (1988)

82. Hoshikawa, H., Koyama, K., Koido, J., Ishibashi, Y.: Characteristics of remote-field eddy current technique. Mater. Eval. **47**(1), 93–97 (1988)

83. Atherton, D.L., Szpunar, B., Sullivan, S.: The application of finite element calculations to the remote field inspection technique. Mater. Eval. **44**(9), 1083–1086 (1987)

84. Nath, S., Lord, W., Sun, Y.S.: Theoretical and experimental studies of the remote field eddy current effect. In: Thompson, D., Chimenti, D. (eds.) Review of Progress in Quantitative Nondestructive Evaluation, vol. 8, pp. 267–274. Springer, Berlin (1989)

85. Kim, D., Udpa, L., Udpa, S.: Remote field eddy current testing for detection of stress corrosion cracks in gas transmission pipelines. Mater. Lett. **58**(15), 2102–2104 (2004)

86. Kasai, N., Matsuzaki, S., Sakamoto, T.: Experimental and analytical study for detectability of the back-side flaws of flat ferromagnetic plates by RFECT. NDT E Int. **44**(8), 703–707 (2011)

87. Clauzon, T., Thollon, F., Nicolas, A.: Flaws characterization with pulsed eddy currents NDT. IEEE Trans. Magn. **35**(3), 1873–1876 (1999)

88. Homberg, C., Henneron, T., Clenet, S.: Stochastic model in eddy current non destructive testing. In: Proc. 2011 14th Eur. Conf. Power Electron. Appl., pp. 1–7 (2011)

89. Kinoshita, K.: Estimation of fatigue evolution of aluminum alloy plated with electroless Ni–CO–P by using electromagnetic impedance method. J. Magn. Magn. Mater. **375**, 80–86 (2015)

90. Fetzer, J., Kurz, S., Lehner, G.: The coupling of boundary elements and finite elements for nondestructive testing applications. IEEE Trans. Magn. **33**(1), 677–681 (1997)

91. Ida, N.: Eddy current nondestructive evaluation—the challenge of accurate modeling. In: DAS—2014 Int. Conf. Dev. Appl. Syst., pp. 97–102 (2014)

92. Sabbagh, H.: A model of eddy-current probes with ferrite cores. IEEE Trans. Magn. **23**(3), 1888–1904 (1987)

93. Sabbagh, L.D., Sabbagh, H.A.: A computer model of eddy-current probe-crack interaction. In: Review of Progress in Quantitative Nondestructive Evaluation, Brunswick (July 1989)

94. Murphy, K., Sabbagh, H.A.: Boundary-integral equations in eddy-current calculations. In: Review of Progress in Quantitative Nondestructive Evaluation 14, pp. 267–274

95. Garcia-Martín, J., Gómez-Gil, J., Vázquez-Sánchez, E.: Nondestructive techniques based on eddy current testing. Sensors **11**, 2525–2565 (2011)

96. Thompson, R.B.: A model for the electromagnetic generation and detection of Rayleigh and Lamb waves. IEEE Trans. Sonics Ultrason. **SU–20**(4), 340–346 (1973)

97. Kawashima, K.: Theory and numerical calculation of the acoustic field produced in metal by an electromagnetic ultrasonic transducer. J. Acoust. Soc. Am. **60**, 1089–1099 (1976)

98. Hao, K.-S., Huang, S.-L., Zhao, W., Duan, R.-J., Wang, S.: Modeling and finite element analysis of transduction process of electromagnetic acoustic transducers for nonferromagnetic metal material testing. J. Cent. South Univ. Technol. **18**(3), 749–754 (2011)

99. Wang, S., Kang, L., Zhichao, L., Zhai, G., Zhang, L.: 3-D modeling and analysis of meander-line-coil surface wave EMATs. Mechatronics **22**(6), 653–660 (2012)

100. Dhayalan, R., Balasubramaniam, K.: A hybrid finite element model for simulation of electromagnetic acoustic transducer (EMAT) based plate waves. NDT E Int. **43**(6), 519–526 (2010)

101. Kim, I.K., Kim, W., Kim, Y.Y.: Magnetostrictive grating with an optimal yoke for generating high-output frequency-tuned SH waves in a plate. Sensors Actuators A Phys. **137**(1), 141–146 (2007)

102. Dutton, B., Boonsang, S., Dewhurst, R.J.: A new magnetic configuration for a small in-plane electromagnetic acoustic transducer applied to laser-ultrasound measurements: Modelling and validation. Sensors Actuators A Phys. **125**(2), 249–259 (2006)

103. Huang, S., Zhao, W., Zhang, Y., Wang, S.: Study on the lift-off effect of EMAT. Sensors Actuators A Phys. **153**(2), 218–221 (2009)

104. Ribichini, R., Nagy, P.B., Ogi, H.: The impact of magnetostriction on the transduction of normal bias field EMATs. NDT E Int. **51**, 8–15 (2012)

105. Grimberg, R., Savin, A., Steigmann, R.: Electromagnetic imaging using evanescent waves. NDT E Int. **46**, 70–76 (2012)
106. Gade, S.O., Weiss, U., Peter, M.A., Sause, M.G.R.: Relation of electromagnetic emission and crack dynamics in epoxy resin materials. J. Nondestruct. Eval. **33**(4), 711–723 (2014)
107. Shibata, T., Hashizume, H., Kitajima, S., Ogura, K.: Experimental study on NDT method using electromagnetic waves. J. Mater. Process. Technol. **161**, 348–352 (2005)
108. Klysz, G., Balayssac, J.P., Ferričres, X.: Evaluation of dielectric properties of concrete by a numerical FDTD model of a GPR coupled antenna—parametric study. NDT E Int. **41**(8), 621–631 (2008)
109. Szczepanik, Z., Rucki, Z.: Field analysis and electrical models of multi-electrode impedance sensors. Sensors Actuators A Phys. **133**(1), 13–22 (2007)
110. Karhunen, K., Seppänen, A., Lehikoinen, A., Monteiro, P.J.M., Kaipio, J.P.: Electrical resistance tomography imaging of concrete. Cem. Concr. Res. **40**, 137–145 (2010)
111. Daneshmand, P.G., Jafari, R.: A 3D hybrid BE–FE solution to the forward problem of electrical impedance tomography. Eng. Anal. Bound. Elem. **37**(4), 757–764 (2013)
112. Zurek, Z.H.: Magnetic contactless detection of stress distribution and assembly defects in constructional steel element. NDT E **38**(7), 589–595 (2005)
113. Augustyniak, M., Usarek, Z.: Discussion of derivability of local residual stress level from magnetic stray field measurement. J. Nondestruct. Eval. **34**, 21 (2014)
114. Usarek, Z., Augustyniak, B., Augustyniak, M., Chmielewski, M.: Influence of plastic deformation on stray magnetic field distribution of soft magnetic steel sample. IEEE Trans. Magn. **50**(4), 1–4 (2014)
115. Usarek, Z., Augustyniak, B., Augustyniak, M.: Separation of the effects of notch and macro residual stress on the MFL signal characteristics. IEEE Trans. Magn. **50**(11), 1–4 (2014)
116. Roskosz, M., Bieniek, M.: Evaluation of residual stress in ferromagnetic steels based on residual magnetic field measurements. NDT E Int. **45**, 55–62 (2012)
117. Pérez-Benítez, J.A., et al.: Analysis of the influence of some magnetizing parameters on magnetic Barkhausen noise using a microscopic model. J. Magn. Magn. Mater. **347**, 51–60 (2013)
118. Pávó, J., Gyimóthy, S.: Adaptive inversion database for electromagnetic nondestructive evaluation. NDT E Int. **40**(3), 192–202 (2007)
119. Sabet-Sharghi, R., Clapham, L., Atherton, D.L., Holden, T.M.: The effect of defect introduction vs. load application sequencing on defect-induced stress distributions in steel samples. NDT E Int. **33**(4), 201–212 (2000)
120. Szielasko, K., Youssef, S., Niese, F., Weikert, M., Sourkov, A., Altpeter, I., Herrmann, H.-G., Dobmann, G., Boller, C.: Multi-method probe design for the electromagnetic characterization of advanced high strength steel. In: Capova, K., et al. (eds.) Studies in Applied Electromagnetics and Mechanics 39: Electromagnetic Nondestructive Evaluation (XVII), pp. 52–59. IOS Press, Amsterdam (2014)
121. Uchimoto, T., Guy, P., Takagi, T., Courbon, J.: Evaluation of an EMAT–EC dual probe in sizing extent of wall thinning. NDT E Int. **62**, 160–166 (2014)
122. Bouchala, T., Abdelhadi, B., Benoudjit, A.: Novel coupled electric field method for defect characterization in eddy current non-destructive testing systems. J. Nondestruct. Eval. **33**(1), 1–11 (2014)
123. Lee, H.-B., Jung, H.-K., Hahn, S.-Y., Chung, J.K.: An inverse analysis for crack identification in eddy current NDT of tubes. IEEE Trans. Magn. **30**(5), 3403–3406 (1994)
124. Putek, P., Crevecoeur, G., Slodicka, M., Gawrylczyk, K., van Keer, R., Dupre, L.: Two-level approach for solving the inverse problem of defect identification in eddy current testing-type NDT. In: IET 8th International Conference on Computation in Electromagnetics (CEM 2011), pp. 1–2 (11–14 Apr 2011)
125. Kim, H.M., Park, G.S.: A study on the estimation of the shapes of axially oriented cracks in CMFL type NDT system. IEEE Trans. Magn. **50**(2), 109–112 (2014)
126. Tamburrino, A., Rubinacci, G.: Fast methods for quantitative eddy-current tomography of conductive materials. IEEE Trans. Magn. **42**(8), 2017–2028 (2006)
127. Yusa, N., Janousek, L., Rebican, M., Chen, Z., Miya, K., Chigusa, N.: Detection of embedded fatigue cracks in Inconel weld overlay and the evaluation of the minimum thickness of the weld overlay using eddy current testing. Nucl. Eng. Des. **236**(18), 1852–1859 (2006)
128. Ossart, F., Hirsinger, L., Billardon, R.: Computation of electromagnetic losses including stress dependence of magnetic hysteresis. J. Magn. Magn. Mater. **196–197**, 924–926 (1999)